

**Downregulation of stanniocalcin 1 is responsible for
sorafenib-induced cardiotoxicity**

Journal:	<i>Toxicological Sciences</i>
Manuscript ID:	TOXSCI-14-0551.R2
Manuscript Type:	Research Article
Date Submitted by the Author:	07-Oct-2014
Complete List of Authors:	<p>Kawabata, Miko; Mie University Graduate School of Medicine, Department of Molecular and Cellular Pharmacology, Pharmacogenomics and Pharmacoinformatics</p> <p>Umemoto, Noriko; Mie University Graduate School of Medicine, Department of Molecular and Cellular Pharmacology, Pharmacogenomics and Pharmacoinformatics; Mie University Graduate School of Medicine, Department of Systems Pharmacology</p> <p>Shimada, Yasuhito; Mie University Graduate School of Medicine, Department of Molecular and Cellular Pharmacology, Pharmacogenomics and Pharmacoinformatics; Mie University Graduate School of Medicine, Department of Systems Pharmacology; Mie University Graduate School of Medicine, Mie University Medical Zebrafish Research Center; Mie University Graduate School of Medicine, Department of Bioinformatics, Mie University Life Science Research Center; Mie University Graduate School of Medicine, Department of Omics Medicine, Mie University Industrial Technology Innovation</p> <p>Nishimura, Yuhei; Mie University Graduate School of Medicine, Department of Molecular and Cellular Pharmacology, Pharmacogenomics and Pharmacoinformatics; Mie University Graduate School of Medicine, Department of Systems Pharmacology; Mie University Graduate School of Medicine, Mie University Medical Zebrafish Research Center; Mie University Graduate School of Medicine, Department of Bioinformatics, Mie University Life Science Research Center; Mie University Graduate School of Medicine, Department of Omics Medicine, Mie University Industrial Technology Innovation</p> <p>Zhang, Beibei; Mie University Graduate School of Medicine, Department of Molecular and Cellular Pharmacology, Pharmacogenomics and Pharmacoinformatics</p> <p>Kuroyanagi, Junya; Mie University Graduate School of Medicine, Department of Molecular and Cellular Pharmacology, Pharmacogenomics and Pharmacoinformatics</p> <p>Miyabe, Masayuki; Mie University Graduate School of Medicine, Department of Clinical Anesthesiology</p> <p>Tanaka, Toshio; Mie University Graduate School of Medicine, Molecular and Cellular Pharmacology; Mie University Graduate School of Medicine, Department of Molecular and Cellular Pharmacology, Pharmacogenomics and Pharmacoinformatics; Mie University Graduate School of Medicine, Department of Systems Pharmacology; Mie University Graduate School of</p>

	Medicine, Mie University Medical Zebrafish Research Center; Mie University Graduate School of Medicine, Department of Bioinformatics, Mie University Life Science Research Center; Mie University Graduate School of Medicine, Department of Omics Medicine, Mie University Industrial Technology Innovation
Key Words:	Gene Expression/Regulation, cardiovascular system < Systems Toxicology, microarray < Methods, siRNA < Methods, bioinformatics < Methods, mechanisms < Systems Toxicology
Society of Toxicology Specialty Section Subject Area:	Cardiovascular Toxicology [106]

SCHOLARONE™
Manuscripts

1
2
3
4
5
6
7
8
9
10
11
12
13
14
15
16
17
18
19
20
21
22
23
24
25
26
27
28
29
30
31
32
33
34
35
36
37
38
39
40
41
42
43
44
45
46
47
48
49
50
51
52
53
54
55
56
57
58
59
60

Downregulation of stanniocalcin 1 is responsible for sorafenib-induced cardiotoxicity

Miko Kawabata^{*,||,2}, Noriko Umemoto^{*,†,2}, Yasuhito Shimada^{*,†,‡,§,¶}, Yuhei Nishimura^{*,†,‡,§,¶},
Beibei Zhang^{*}, Junya Kuroyanagi^{*}, Masayuki Miyabe^{||} and Toshio Tanaka^{*,†,‡,§,¶,1}

*Department of Molecular and Cellular Pharmacology, Pharmacogenomics and
Pharmacoinformatics, Mie University Graduate School of Medicine, 2-174 Edobashi, Tsu,
Mie 514-8507, Japan

†Department of Systems Pharmacology, Mie University Graduate School of Medicine, 2-174
Edobashi, Tsu, Mie 514-8507, Japan

‡Mie University Medical Zebrafish Research Center, 2-174 Edobashi, Tsu, Mie 514-8507,
Japan

§Department of Bioinformatics, Mie University Life Science Research Center, 2-174
Edobashi, Tsu, Mie 514-8507, Japan

¶Department of Omics Medicine, Mie University Industrial Technology Innovation, 2-174
Edobashi, Tsu, Mie 514-8507, Japan

||Department of Clinical Anesthesiology, Mie University Graduate School of Medicine, 2-174
Edobashi, Tsu, Mie 514-8507, Japan

¹Corresponding author: Toshio Tanaka, 2-174 Edobashi, Tsu, Mie 514-8507, Japan

²These authors contributed equally to this work

E-mail: tanaka@doc.medic.mie-u.ac.jp

Tel: 81-59-231-5411

Fax: 81-59-232-1765

Running title: Cardiotoxicity of sorafenib

Abstract

Sorafenib is associated with adverse cardiac effects, including left ventricular dysfunction. However, the precise mechanism remains unclear. Here, we aimed to establish the genes responsible for this cardiotoxicity using zebrafish and human cardiomyocytes. Fluorescent cardiac imaging using pigmentless zebrafish with green fluorescent protein hearts revealed that the ventricular dimensions of the longitudinal axis with sorafenib were significantly shorter than those of the control group. Transcriptome analysis of their hearts revealed that stanniocalcin 1 (*stc1*) was downregulated by sorafenib. *stc1* knockdown in zebrafish revealed that reduction of *stc1* decreased the longitudinal dimensions of zebrafish ventricles, similar to that which occurs during sorafenib treatment. *STC1* downregulation and cytotoxicity were also seen in human cardiomyocytes exposed to sorafenib. To clarify the molecular function of *stc1* in sorafenib-induced cardiotoxicity, we focused on oxidative stress in cardiomyocytes treated with sorafenib. Reactive oxygen species (ROS) production significantly increased in both species of human cardiomyocytes and zebrafish exposed to sorafenib and *STC1* knockdown compared with the controls. Finally, we found that forced expression of *stc1* normalized impairment, decreasing the longitudinal dimensions in zebrafish treated with sorafenib. Our study demonstrated that *STC1* plays a protective role against ventricular dysfunction and ROS overproduction, which are induced by sorafenib treatment. We discovered for the first time that *STC1* downregulation is responsible for sorafenib-induced cardiotoxicity through activated ROS generation.

Keywords: sorafenib, stanniocalcin 1, cardiotoxicity, zebrafish, reactive oxygen species

Introduction

Cardiotoxicity is one of the most significant adverse effects of cancer treatment, and is responsible for considerable morbidity and mortality (Adão *et al.*, 2013). Cardiac function is maintained by an intricate cycle of molecular signaling events that significantly overlap the signaling pathways of tumor growth. For example, many protein kinases are constitutively active in cancer cells, through mutations, overexpression, or translocation (Force *et al.*, 2007). However, the use of certain chemotherapeutics for the treatment of cancer is associated with a risk of adverse effects on cardiac function (Force, Krause and Van Etten, 2007). These kinase inhibitors can be cardiotoxic in a subset of patients (Force and Kolaja, 2011). With consideration to the therapeutic efficacy of these small molecular inhibitors, it is crucial to clarify the precise mechanism of drug-induced cardiotoxicity. Sorafenib is the first oral multikinase inhibitor that can inhibit v-raf-1 murine leukemia viral oncogene homolog 1 (RAF1), v-raf murine sarcoma viral oncogene homolog B1 (BRAF), fms-like tyrosine kinase (FLT)4, also known as vascular endothelial growth factor receptor (VEGFR)3, FLT3, v-kit Hardy-Zuckerman 4 feline sarcoma viral oncogene homolog (KIT), and platelet-derived growth factor receptor (PDGFR). The safety and efficacy of sorafenib in patients with advanced hepatocellular carcinoma (HCC) was demonstrated in two phase III randomized, double-blind, placebo-controlled trials, the Sorafenib HCC Assessment Randomized Protocol (SHARP) and Asia-Pacific (AP) trials (Cheng *et al.*, 2009; Llovet *et al.*, 2008a), thereby establishing sorafenib as the standard systemic therapy for advanced HCC (Bruix *et al.*, 2011; Llovet *et al.*, 2008b; Miyahara *et al.*, 2014). The left ventricular ejection fraction (LVEF) was found to be below the lower limit of normal at the time of “cardiac events” in 21.4 % of patients, but the significance of this is entirely unclear because baseline LVEF was not determined. The study that examined baseline and serial LVEF determinations in patients on sorafenib reported that mean LVEF declined by only 0.8-1.2 EF percent (Tolcher *et al.*, 2010,

1
2
3 2011; Cheng *et al.*). These authors reported that the effects on LVEF were modest and were
4
5 unlikely to be of clinical significance, but 13 % of patients had significant declines in EF (\geq
6
7 10 EF points). In the study by Schmidinger *et al.* (Schmidinger *et al.*, 2008), the incidence of
8
9 reduced LVEF for sorafenib was reported as 5%. Several mechanisms of sorafenib-induced
10
11 cardiotoxicity have been reported, including inhibition of the RAF/mitogen-activated protein
12
13 kinase kinase (MEK)/extracellular signal-regulated kinase (ERK) pathway (Mellor *et al.*,
14
15 2011; Cheng *et al.*, 2011), and disruption of VEGF–VEGFR signaling through inhibition of
16
17 circulating VEGF and inhibition of PDGFRs (Hasinoff and Patel, 2010). Recently, Cheng *et*
18
19 *al.* reported that sorafenib-induced cardiotoxicity may be preventable by activation of
20
21 α -adrenergic signaling. Phenylephrine can activate ERK independently of RAF (Cheng *et al.*,
22
23 2011). Further studies are required to give more options for the prevention of
24
25 sorafenib-induced cardiotoxicity.
26
27
28
29

30 Zebrafish have emerged as a useful animal model to clarify the molecular
31
32 mechanisms of various cardiac diseases, including drug-induced cardiotoxicity (Lal *et al.*,
33
34 2013). Zebrafish in which a certain gene product associate with human heart failure was
35
36 reduced showed a decrease in EF, similar to the human phenotype (Seguchi *et al.*, 2007). We
37
38 have also developed a fluorescent cardiac imaging of pigmentless zebrafish heart that can
39
40 assess the cardiac function in various physiological and pathophysiological situations
41
42 (Umemoto *et al.*, 2013). In the present study, we applied functional cardiac imaging and
43
44 transcriptome analysis to zebrafish to clarify the molecular mechanism of sorafenib-induced
45
46 cardiotoxicity. These analyses, combined with the validation studies using human
47
48 cardiomyocytes, revealed that downregulation of *STC1*, a gene that has cardioprotective
49
50 function (Koizumi *et al.*, 2007; Liu *et al.*, 2012), is responsible for sorafenib-induced
51
52 cardiotoxicity.
53
54
55
56
57
58
59
60

MATERIALS AND METHODS

This study was approved by the Ethics Committee of Mie University School of Medicine, Japan, and involved the use of zebrafish embryos as experimental animals. Animal care was also in accordance with the NIH guidelines.

Experimental animals.

We obtained a pigmentless zebrafish line *nacre* (Lister *et al.*, 1999) from Zebrafish International Resource Center (ZIRC; Eugene, OR, USA) and a transgenic zebrafish line SAG4A (Kawakami *et al.*, 2004) expressing enhanced green fluorescent protein (GFP) in the heart from the National Institute of Genetics (Mishima, Japan). We crossed *nacre* and SAG4A to create MieKomachi 009 (MK009) (Supplementary, Figure S1A). MK009 were bred and maintained as described by Westerfield (Westerfield, 2007). Zebrafish were raised at $28.5 \pm 0.5^\circ\text{C}$ with a 14 /10 h light/dark cycle. Embryos were obtained via natural mating and cultured in Egg Water (1.5 mL stock salts added to 1 l distilled water).

Sorafenib exposure.

We filled a 6-well plate (Falcon, New York, NY, USA) with 2 ml egg water per well (10 fish of 3 days post fertilization (dpf) in each of 6 baskets). Fifty zebrafish per group were analyzed. We administered sorafenib (1 or 3 μM) or 1% dimethyl sulfoxide (DMSO) to MK009 from 3 to 10 dpf, and changed the medium every day. MK009 were immobilized by placing them on 3% methylcellulose (Sigma-Aldrich, St. Louis, MO, USA) on a glass slide (Matsunami, Tokyo, Japan). Images were captured using a biological microscope (MZF16A; Leica, Wetzlar, Germany) with a digital camera (DP2; Olympus, Tokyo, Japan). The criterion for survival was the presence of cardiac contractions.

Cardiac imaging analysis.

We administered 1 μ M sorafenib or 1% DMSO to MK009 from 72 to 96 or 120 hours post-fertilization (hpf). MK009 were immobilized by placing them on 3% methylcellulose in a microscopy chamber (u-Slide 8 well uncoated; ibidi, Munich, Germany) without anesthesia. After they were adjusted to a “head left” position, movie files were recorded on Image Xpress MICRO (Molecular Devices, Sunnyvale, CA, USA), at a frame rate of 33.5 frames/second for approximately 6 s.

We used MacBiophotonics Image J (NIH, Bethesda, MD, USA) (Collins, 2007) to process the original records for the measurement of cardiac performance using GFP heart imaging, as described by Umemoto *et al.* (Umemoto *et al.*, 2013). To make M-mode images in the longitudinal (long) or short axes of the ventricle, the intersection of horizontal and vertical lines was positioned at the center of mass according to our preliminary experiment (Umemoto *et al.*, 2013). The ventricular end-systolic dimension (VDs) and the ventricular end-diastolic dimension (VDd) were measured from the M-mode images (Supplementary, Figure S1B). VDs and VDd were obtained at maximal inward and outward excursions, respectively, of the ventricular wall in the M-mode images. We measured VDs and VDd along the short axis (short VDs and short VDd) and the longitudinal axis (long VDs and long VDd). For each determination, five diastoles and systoles were analyzed. The end-diastolic volume (EDV) and end-systolic volume (ESV) were calculated using the formula for a prolate spheroid ($4 \times a \times b^2/3$) (Jacob *et al.*, 2002). The stroke volume (SV) was obtained by subtracting the ESV from the EDV. The EF was calculated as SV/EDV and the percentage fractional shortening (FS) was calculated from the formula: $100 \text{ (short VDd} - \text{short VDs)}/\text{short VDd}$.

cDNA microarray analysis.

MK009 treated with 1 μ M sorafenib or 1% DMSO from 72 to 96 hpf were anesthetized using

1
2
3 0.05% 2 phenoxy-ethanol (Wako Pure Chemicals, Osaka, Japan). The hearts were surgically
4
5 isolated using a fluorescence microscope. Twenty hearts were collected in a tube containing
6
7 RNAlater (Life Technologies, Carlsbad, CA, USA). Four biological replicates were prepared
8
9 for each group. Total RNA was extracted using the RNAqueous-Micro Kit (Life
10
11 Technologies), qualified by Agilent Bioanalyzer 2100 (Agilent Technologies, Santa Clara,
12
13 CA, USA), and quantified using a spectrophotometer (Nano Drop ND-100; Wilmington, DE,
14
15 USA). Seven hundred nanograms of total RNA was converted into labeled cRNA using the
16
17 Low Input Quick Amp Labeling Kit (Agilent Technologies). Cy3-labeled cRNA (1.65 µg)
18
19 was hybridized to Agilent Zebrafish Whole Genome Oligo Microarrays (G2519F) according
20
21 to the manufacturer's protocol. The hybridized microarrays were scanned by DNA
22
23 Microarray Scanner (G2565BA; Agilent Technologies) and analyzed using Feature Extraction
24
25 software (Agilent Technologies). The data were normalized using Agi4x44PreProcess.
26
27 RankProd analysis was performed using Bioconductor to identify differentially expressed
28
29 genes between two groups by calculating the false discovery rate (FDR). Differentially
30
31 expressed genes (FDR <10%) were then converted to human orthologs using the Life Science
32
33 Knowledge Bank (World Fusion, Tokyo, Japan). These genes were subjected to Pathway
34
35 Studio, which is a program used to visualize and analyze biological pathways and gene
36
37 regulation networks. This program includes the ResNet database of >500,000 functional
38
39 relationships between genes and between genes and functional entities such as heart failure.
40
41 The microarray dataset has been deposited in GEO as GSE61155.
42
43
44
45
46
47
48

49 *Cell preparations.*

50
51 Human adult primary cardiomyocytes were purchased (PromoCell, Heidelberg, Germany)
52
53 and cultured according to the manufacturer's instructions. Cardiomyocytes were grown for 2
54
55 weeks in a medium consisting of Myocyte Growth Medium Kit (PromoCell) supplemented
56
57
58
59
60

1
2
3 with 5% fetal calf serum, epidermal growth factor (0.5 ng/ml), basic fibroblast growth factor
4
5 (2 ng/ml), and insulin (5 µg/ml) at 37°C in a 5% CO₂ humidified incubator, and the medium
6
7 was changed every day.
8
9

10 11 ***siRNA transfection.***

12
13 Stealth siRNAs (Stealth RNAi Negative Control Med GC [12935-300] and Stealth RNAi for
14
15 STC1 [STC1siRNA1:HSS110297 and STC1siRNA2:HSS186139]) were purchased from Life
16
17 Technologies, and were denoted as NCsiRNA and STC1siRNA1-2, respectively. Three
18
19 biological replicates were prepared for each group. The sequences of siRNAs used in this
20
21 study are shown in Supplementary Table S1. Cultured cells were transfected with siRNAs (50
22
23 nM final concentration) using Lipofectamine RNAiMAX (Life Technologies) according to the
24
25 manufacturer's protocol.
26
27
28
29
30
31

32 ***Quantitative PCR analysis.***

33
34 Total RNA from heart tissues and whole body of zebrafish was purified as described above.
35
36 Total RNA from human cardiomyocytes was also purified using the RNeasy Mini Kit
37
38 (Qiagen, Valencia, CA, USA). First-standard cDNA was prepared with 200 ng total RNA and
39
40 used to generate cDNA using an iScript Select cDNA Synthesis Kit (Bio-Rad, Hercules, CA,
41
42 USA). Quantitative (q)PCR was performed using an ABI Prism 7300 (Life Technologies)
43
44 with SYBR Green Real-time PCR Master Mix Plus (Toyobo, Osaka, Japan). The thermal
45
46 cycling conditions comprised an initial step at 95°C for 1 min followed by 40 cycles of 95°C
47
48 for 15 s, 60°C for 15 s and 72°C for 45 s. The sequences of primers used in this study are
49
50 shown in Supplementary Table S1. Gene expression levels were calculated using the standard
51
52 curve method.
53
54
55
56
57
58
59
60

Injections of morpholino and/or stc1 mRNA.

The *stc1* antisense morpholino oligonucleotides (MOs) and standard control MO were purchased from Gene Tools (Philomath, OR, USA). The *stc1* antisense MO was designed to splice out the second exon of *stc1* (zgc:153307). The sequences of MOs used in this study are shown in Supplementary Table S1.

The zebrafish *stc1* (amino acids 1–250) obtained from ZGC clone 153307 (Source BioScience, Nottingham, UK) was subcloned into the *EcoRI* and *XbaI* sites of the plasmid pCS2P+ (Addgene, Cambridge, MA, USA). The sequence of the construct was confirmed by DNA sequencing (FASMAC, Kanagawa, Japan). The sequence containing full-length cDNA for *stc1* was amplified by PCR using the primer pairs: SP6 and T3. The PCR product was used as the template for RNA synthesis. The *stc1* mRNA was synthesized using the mMessage mMachine transcription kit for SP6 RNA polymerase (Life Technologies).

For knockdown of *stc1*, a solution containing 0.3 mM *stc1* MO was injected into 1–4-cell stage embryos. A solution containing 0.3 mM control MO was also injected into zebrafish as a control. For the rescue experiment, a solution containing mRNA (0.87 μ M) with or without 0.3 mM *stc1* MO was injected into 1–4-cell stage embryos. These embryos were raised in Egg Water at 28.5°C until 96 hpf.

ROS measurement.

In zebrafish experiments, we administered 1 μ M sorafenib or 1% DMSO to MK009 from 72 to 74 hpf. Dihydroethidium (DHE) (Life Technologies) was dissolved in DMSO and used at a final concentration of 10 μ M in Egg Water in the presence of 0.1% DMSO. Zebrafish were incubated with DHE for 15 min in the dark chamber (Ogrunc *et al.*, 2014), rinsed in Egg Water twice, and anesthetized using 2 phenoxy-ethanol, then immediately imaged under a Nikon stereomicroscope SMZ 25 (Tokyo, Japan) equipped with filters for DS-Red. Zebrafish

1
2
3 fluorescent intensity of zebrafish whole body was quantified using the MacBiophotonics
4
5 Image J (NIH).
6

7 Following 0.3 μM sorafenib or vehicle administration for 1 h, cultured cardiomyocytes were
8
9 incubated with cell-permeable redox-sensitive fluorophore CellRox Deep Red detection
10
11 reagent (Life Technologies) in a microscopy chamber (u-Slide 8 well uncoated; ibidi, Munich,
12
13 Germany), at a concentration of 5 μM for 30 min. Hoechst 33342 dye (10 μM ; Dojin,
14
15 Kumamoto, Japan) was used to visualize the nuclei. Cardiomyocytes were washed with warm
16
17 PBS twice. Cell images were acquired using Image Xpress MICRO high content screening
18
19 system (Molecular Devices). Cell fluorescence was quantified using the accompanying
20
21 software. Three biological replicates were prepared for each group. For determination of ROS,
22
23 N-acetyl-cysteine (ENZO Life Science, Farmingdale, NY, USA), a ROS scavenger, was used
24
25 to cardiomyocytes at the concentration of 0.5 mM for 1 h prior to sorafenib administration.
26
27
28
29
30
31

32 ***Statistical analysis.***

33
34 Results are expressed as mean \pm standard error. Differences among groups were tested for
35
36 statistical significance using the unpaired Student's *t* test, and $P < 0.05$ was considered
37
38 significant. For multiple comparisons, one-way analysis of variance followed by the
39
40 Tukey–Kramer procedure was used. All statistical analyses were conducted using Statcel 2
41
42 software (OMS, Tokyo, Japan).
43
44
45
46

47 **RESULTS**

48 ***Sorafenib cardiotoxicity in zebrafish line MK009***

49
50 To assess the cardiotoxicity of sorafenib in zebrafish, we created a novel zebrafish line
51
52 MK009 by crossing *nacre* and SAG4A. *nacre* is a zebrafish mutant with a pigmentless body
53
54 due to lack of the *mitfa* gene (Lister *et al.*, 1999). SAG4A is a transgenic zebrafish in which
55
56
57
58
59
60

1
2
3 GFP is selectively expressed in the heart (Kawakami *et al.*, 2004). MK009 is an attractive
4
5 model for cardiac imaging, because the fluorescent heart can be clearly observed in the
6
7 pigmentless body (Supplementary, Figure S1A).
8

9
10 The maximum plasma concentration of sorafenib after a 28-day cycle in patients
11
12 receiving 400 mg, 2 times per day was 8.5 μM and the trough concentration was 6.4 μM in
13
14 phase 1 clinical trials (Cheng, *et al.* 2011; Tolcher, *et al.* 2010; Stumberg, *et al.* 2007). Thus,
15
16 in the following experiments we choose the concentrations of 1 and 3 μM . The survival rate
17
18 of zebrafish treated with 3 μM sorafenib was decreased to ~20% at 5 dpf (Figure 1A, black
19
20 solid line). In addition, zebrafish exposed to 3 μM sorafenib showed some noticeable body
21
22 malformations including a curved body shape, and an uninflated swim bladder (Figure 1B).
23
24 No zebrafish were alive in the 3 μM sorafenib group on 6 dpf. Zebrafish treated with 1 μM
25
26 sorafenib did not show any decrease in survival rate until 6 dpf (Figure 1A, gray solid line) or
27
28 any external malformation (Figure 1B) until 5 dpf.
29
30

31
32 We then assessed the cardiac function in zebrafish treated with 1 μM sorafenib using
33
34 the quantitative fluorescent cardiac imaging that we have developed (Umemoto, *et al.* 2013)
35
36 (Supplementary Figure S1B). Because 3 μM sorafenib caused significant mortality by 120 hpf,
37
38 1 μM sorafenib was used for the remaining experiments. At 96 hpf (24 h exposure), both long
39
40 VDD and VDs in zebrafish treated with sorafenib were significantly ($P < 0.05$) shorter than
41
42 those of the control group (Figure 2A). However, the calculated ejection fraction (EF) and
43
44 fractional shortening (FS) were not significantly different between zebrafish with sorafenib
45
46 treatment and those of control group (Figure 2B). At 120 hpf (48 h exposure), long VDs in
47
48 zebrafish treated with sorafenib were significantly ($P < 0.01$) longer than those of the control
49
50 group (Figure 2C). Both the calculated ejection fraction (EF) and fractional shortening (FS) in
51
52 zebrafish with sorafenib treatment were significantly ($P < 0.01$) decreased compared with the
53
54 control group (Figure 2D). These results suggest that 1 μM sorafenib treatment from 72 to 96
55
56
57
58
59
60

1
2
3 hpf induced selectivity longitudinal impairment with preserved both EF and FS of zebrafish
4
5 ventricle.
6
7
8

9
10 ***Sorafenib reduces expression of *stc1* in heart of MK009***

11
12 To clarify the molecular mechanism of sorafenib-induced cardiotoxicity by eliminating the
13 secondary effect of ventricular dysfunction, we performed transcriptome analysis of hearts
14 isolated from zebrafish with or without exposure to 1 μ M sorafenib for 24 h. Using a
15 commercially available DNA microarray system, we analyzed the expression of 21,383
16 probes that were reliably expressed in the hearts (GSE 61155) and identified 215 genes
17 significantly (false discovery rate; FDR <10%) dysregulated between hearts with and without
18 sorafenib treatment (Supplementary, Table S2). 56 and 159 genes were significantly down-
19 and upregulated, respectively, in the heart with sorafenib treatment.
20
21
22
23
24
25
26
27
28

29
30 To identify genes that might be relevant to sorafenib-induced cardiotoxicity, we
31 performed a bioinformatics approach using the 215 genes dysregulated by sorafenib treatment
32 in MK009 and Pathway Studio, a bioinformatics software. First, we selected “heart failure” as
33 a functional entity in the Pathway Studio and identified 32 genes that were linked to heart
34 failure (Supplementary, Figure S2A). It has been shown that ERK (MAPK1 and MAPK3) are
35 involved in sorafenib-induced cardiotoxicity (Cheng *et al.*, 2011; Hasinoff and Patel, 2010).
36 Therefore, we selected “MAPK1” and “MAPK3” as molecular entities in the Pathway Studio
37 and identified 14 genes whose expression was regulated by both MAPK1 (ERK2) and
38 MAPK3 (ERK1) (Supplementary, Figure S2B). Two and 12 genes were down- and
39 upregulated in the hearts with sorafenib treatment, respectively. It has been reported that
40 sorafenib inhibits the phosphorylation of MAPK1 and MAPK3 and the function of these
41 ERKs. We focused on *stc1* because the expression of *stc1* was positively regulated by ERK
42 (Nguyen *et al.*, 2009) and VEGF (Holmes and Zachary, 2008) signaling. We performed
43
44
45
46
47
48
49
50
51
52
53
54
55
56
57
58
59
60

1
2
3 quantitative polymerase chain reaction (qPCR) to confirm the downregulation of *stc1* in the
4 hearts of zebrafish exposed to sorafenib. As shown in Figure 3A, the expression level of *stc1*
5 was significantly ($P < 0.05$) lower than that of the control heart.
6
7

8
9 We performed qPCR to confirm the downregulation of *STC1* exposed to 0.3 μ M sorafenib or
10 vehicle for 24 h. As shown in Figure 3B, the expression level of *STC1* in human
11 cardiomyocytes exposed to sorafenib was significantly ($P < 0.05$) lower than that exposed to
12 the vehicle.
13
14
15
16
17
18
19

20 ***Reduction of stc1 impairs cardiac function in MK009***

21
22 We examined whether the reduction of *stc1* affected cardiac function in MK009. To knock
23 down *stc1* expression, zebrafish embryos were injected with *stc1* MO. We conducted *stc1*
24 knockdown using splicing inhibitor MO, and confirmed the gene knockdown level by qPCR.
25 ($P < 0.01$ sorafenib versus vehicle, Figure 3C). Functional cardiac imaging at 96 hpf revealed
26 that both long VDs and long VDd in *stc1* morphant (Figure 3D, black bar) were significantly
27 shorter than those in control zebrafish that were injected with control MO (Figure 3D, white
28 bar). The calculated EF and FS were not significantly different between *stc1* morphant and
29 control zebrafish (Figure 3E). The reduction of both long VDs and long VDd in *stc1*
30 morphant at 96 hpf was similar to that in zebrafish exposed to sorafenib from 72 to 96 hpf
31 (Figure 2A).
32
33
34
35
36
37
38
39
40
41
42
43
44

45 To confirm whether the decrease in long VDs and long VDd in *stc1* morphant was
46 caused by reduced expression of *stc1*, zebrafish embryos were co-injected with *stc1* MO and
47 *stc1* mRNA. *stc1* MO was designed to bind to the junction of the first intron and second exon
48 of *stc1*, thus *stc1* MO was not likely to bind to *stc1* mRNA. Therefore, *stc1* mRNA should be
49 translated into *stc1* protein without interference from *stc1* MO. Functional cardiac imaging at
50 96 hpf revealed that both long VDs and long VDd were significantly increased in zebrafish
51
52
53
54
55
56
57
58
59
60

1
2
3 co-injected with *stc1* MO and *stc1* mRNA (Figure 3D, gray bar) compared with those of *stc1*
4 morphant (Figure 3D black bar). The calculated EF and FS were not statistically different
5 among the three groups (Figure 3E). These results suggest that reduction of *stc1* could cause
6 dysregulation of ventricular dimensions in zebrafish.
7
8
9
10

11 ***Sorafenib-induced STC1 reduction causes ROS overproduction in human cardiomyocytes***

12
13
14 It has been reported that sorafenib increases ROS generation in human cancer cells (Coriat *et*
15 *al.*, 2012; Fumarola *et al.*, 2013) and that *STC1* suppresses ROS generation induced by
16 angiotensin II in rodent cardiomyocytes (Liu *et al.*, 2012). To examine the relationship
17 between *stc1* and cardiotoxicity, we observed accumulation of ROS throughout the body of
18 zebrafish treated with 1 μ M sorafenib for 2 h (Figure 4A). ROS were detected in vivo by
19 adapting a protocol based on DHE. ROS generation of zebrafish treated with sorafenib was
20 significantly increased in vehicle treated zebrafish (Figure 4B). NAC, a known scavenger of
21 ROS, inhibited the increase in ROS level by sorafenib treatment (Figure 4B). To examine
22 whether reduction of *stc1* affected ROS generation, zebrafish embryos were injected with 0.3
23 mM *stc1* MO or 0.3 mM control MO (Figure 4C). ROS generation was significantly increased
24 in zebrafish injected with *stc1* MO compared with control MO (Figure 4D and E) and with
25 *stc1* MO + *stc1* mRNA (Figure 4E).
26
27
28
29
30
31
32
33
34
35
36
37
38
39
40
41
42

43 Furthermore, to validate the involvement of *STC1* in sorafenib-induced cardiotoxicity in
44 humans, we conducted an in vitro study using human cardiomyocytes. To examine whether
45 sorafenib induces ROS generation in cardiomyocytes, we treated human cardiomyocytes with
46 or without 0.3 μ M sorafenib for 1 h and assessed the ROS generation using fluorescent
47 imaging. As shown in Figure 5A and 5B, ROS generation was significantly ($P < 0.05$)
48 increased in human cardiomyocytes exposed to sorafenib compared with that in the control.
49
50
51
52
53
54
55
56 To examine whether reduction of *STC1* could affect ROS generation, human cardiomyocytes
57
58
59
60

1
2
3 were transfected with *STC1* or negative control (NC) siRNA. ROS generation was
4
5 significantly ($P < 0.05$) increased in human cardiomyocytes transfected with *STC1*siRNA
6
7 compared with NC siRNA (Figure 5C and 5D). As shown Figure 5E, the expression of *STC1*
8
9 in human cardiomyocytes transfected with *STC1*siRNA were significantly ($P < 0.05$) lower
10
11 than that of NCsiRNA.
12

13 14 15 16 ***Forced expression of *stc1* reverses sorafenib-induced cardiotoxicity***

17
18 We investigated whether forced expression of *stc1* reversed sorafenib-induced cardiotoxicity
19
20 in zebrafish. Zebrafish embryos were injected with or without *stc1* mRNA and treated with or
21
22 without 1 μ M sorafenib from 72 to 96 hpf. Functional cardiac imaging at 96 hpf revealed that
23
24 both long VDs and long VDd in zebrafish without *stc1* mRNA injection and with sorafenib
25
26 treatment (Figure 6A, black bar) were significantly shorter than those in zebrafish without
27
28 *stc1* mRNA and sorafenib (Figure 6A, white bar) and zebrafish with *stc1* mRNA and without
29
30 sorafenib (Figure 6A, gray bar). Both long VDs and long VDd in zebrafish with *stc1* mRNA
31
32 injection and sorafenib treatment (Figure 6A, shaded bar) did not differ significantly from
33
34 those in zebrafish without *stc1* mRNA and sorafenib (Figure 6A, white bar). There was no
35
36 significant difference in the calculated EF and FS among the 4 groups (Figure 6B).
37
38 Furthermore, forced expression of *stc1* mRNA suppressed sorafenib-induced ROS generation
39
40 (Figure 6C). These results suggest that reduction of *stc1* could be responsible for
41
42 sorafenib-induced cardiotoxicity.
43
44
45
46
47
48

49 50 **DISCUSSION**

51
52 The pigmentless zebrafish line MK009 was developed to allow quantitative observation of
53
54 heart function that is highlighted by GFP. Owing to fluorescent cardiac image analysis of
55
56 MK009 using a high-content imager with LED illumination as an inverted fluorescent
57
58
59
60

1
2
3 microscope, we were able to demonstrate that the ventricular dimension of the longitudinal
4 axis decreased with preserved EF and FS in zebrafish treated with 1 μ M sorafenib from 72 to
5 96 hpf. This cardiac functional imaging is an innovative way to detect clearly the target
6 tissues, if the intensity of fluorescence in the tissues is as weak as that of cardiac GFP in
7 MK009, because the LED illumination of the high-content imager is brighter than the halogen
8 illumination of simple manual microscopes. We also found that the longitudinal dimension
9 increased with reduced EF and FS in zebrafish treated with 1 μ M sorafenib from 72 to 120
10 hpf (Figure 2D). These results were consistent with a previous study that reported a
11 significant increase in the end-systolic dimension of both ventricular axes and decreased FS
12 after administration of 0.5 μ M sorafenib from 48 to 120 hpf (Cheng *et al.*, 2011). In a
13 previous clinical study, a reduction in the ventricular dimension of the longitudinal axis was
14 detected in patients with early-stage heart failure induced by sorafenib (Di Salvo *et al.*, 2011).
15 This is in good agreement with our study that showed reduced longitudinal dimension in
16 zebrafish treated with sorafenib from 72 to 96 hpf. These results suggest that the zebrafish
17 cardiotoxic model treated with 1 μ M sorafenib for 24 hours showed selective longitudinal
18 ventricular dysfunction with preserved EF and FS, which mimicked sorafenib-induced
19 cardiotoxicity in humans.

20
21 To establish the mechanism of cardiotoxicity as on-target and off-target effects, we
22 aimed to identify differentially expressed genes in the sorafenib-induced cardiotoxic model.
23 Sorafenib inhibited RAF1, which is coded by mitogen activated protein kinase kinase kinase
24 (MAP3K). Once activated, RAF1 can phosphorylate the dual specificity protein kinases
25 MEK1/2 to activate them. These in turn phosphorylate the serine/threonine specific protein
26 kinases ERK1/2 to activate them (Roux and Blenis, 2004). Activated ERKs are effectors of
27 cell physiology and control gene expression involved in the regulation of cell cycle
28 progression, proliferation, cytokinesis, transcription, differentiation, senescence, and
29

1
2
3 apoptosis (Orphanos *et al.*, 2009). RAF1 inhibits two proapoptotic kinases, apoptosis
4
5 signal-regulating kinase (ASK)1 and mammalian sterile 20-like kinase (MST)2, which are
6
7 important in oxidative-stress-induced injury. Deletion of RAF1 gene in the heart leads to a
8
9 dilated, hypocontractile heart with increased cardiomyocyte apoptosis (Feng *et al.*, 2013).
10

11
12 In the present study, to determine an accurate gene expression profile in the
13
14 sorafenib-induced cardiotoxic model, we performed transcriptome analysis using a cDNA
15
16 microarray from a small amount of heart tissue (20 hearts per group). In a previous
17
18 transcriptome analysis of heart tissue in zebrafish (Burns and MacRae, 2006), the authors
19
20 used 500 isolated hearts of zebrafish larvae for each condition of their microarray experiment.
21
22 However, their technology for heart isolation using a micropipette carries a risk of including
23
24 noncardiac tissue in the samples. In our study, we developed a method to isolate cardiac tissue
25
26 easily from zebrafish larvae by using microsurgical scissors and preparing RNA samples
27
28 extracted from 20 hearts for each DNA chip. We analyzed the expression data using Gene Set
29
30 Enrichment Analysis (GSEA) by Pathway Studio to find gene ontology (GO) associated with
31
32 the 215 genes whose expression levels were altered by sorafenib treatment in zebrafish. From
33
34 the DNA microarray analysis, we identified 14 genes whose expression was regulated by both
35
36 MAPK1 and MAPK3, and was linked to heart failure using a bioinformatics approach of
37
38 Pathway Studio. Two and 12 genes were down- and upregulated in the hearts with sorafenib
39
40 treatment, respectively (Supplementary, Figure S2B).
41
42
43
44

45 We focused on oxidative stress as a potential off-target effect of sorafenib. It is
46
47 known that sorafenib can provoke rapid generation of various ROS in two HCC cell lines
48
49 (HepG2 and Hepa 1.6) and human umbilical vein endothelial cells, and exerts dose-dependent
50
51 cytostatic and cytotoxic effects (Chiou *et al.*, 2009 ; Jacob *et al.*,2002). Additionally, it is
52
53 recognized that anticancer agents, such as adriamycin, induce dose-limiting cardiotoxicity.
54
55 There is a consensus that this toxicity is related to the induction of ROS. Induction of ROS in
56
57
58
59
60

1
2
3 the heart by adriamycin occurs via redox cycling of the drug at complex I of the electron
4 transport chain (Berthiaume and Wallace, 2007). We hypothesized that sorafenib might induce
5 the overproduction of ROS in the heart. In fact, Hasinoff and Patel reported that sorafenib
6 treatment of neonatal rat cardiomyocytes caused dose-dependent damage and increased
7 oxidative activity at therapeutically relevant concentrations (Hasinoff and Patel, 2010). A
8 previous clinical study also reported that serum levels of advanced oxidation protein products
9 on ROS in patients with HCC treated with sorafenib were increased after 15 days treatment
10 (Coriat *et al.*, 2012). However, these authors could not clarify the mechanism of
11 sorafenib-induced cardiotoxicity. As a result of the GSEA in our study, *STC1* was classified in
12 “ROS generation” in the GO list of cell processing categories (Supplementary, Table S3). To
13 the best of our knowledge, this is the potential mechanism of sorafenib-induced cardiotoxicity.
14 Here, we demonstrated overproduction of ROS and reduction of *stc1* in zebrafish treated with
15 1 μ M sorafenib for 2 and 24 hours, respectively. Overproduction of ROS and reduction of
16 *STC1* in human cardiomyocytes treated with 0.3 μ M sorafenib for 1 h were also shown in our
17 study. We also observed a cytotoxic phenotype in human cardiomyocytes treated with 1 μ M
18 sorafenib for 24 h (data not shown). Moreover, *STC1* knockdown in zebrafish and human
19 cardiomyocytes significantly increased ROS production compared with the cardiomyocytes
20 treated with vehicle. Our results suggest that induction of ROS by sorafenib in zebrafish and
21 human cardiomyocytes is associated with reduction of *STC1*.

22
23
24
25
26
27
28
29
30
31
32
33
34
35
36
37
38
39
40
41
42
43
44
45 *STC1* is a glycoprotein hormone involved in calcium/phosphate homeostasis, which
46 was originally discovered as a secretory hormone of the corpuscle of Stannius, an endocrine
47 gland of teleosts (Jiang *et al.*, 2000). This gene is evolutionarily highly conserved, with the
48 first 202 amino acids showing 90% similarity between human *STC1* (NM-003155) and
49 zebrafish *stc1* (NM-001045457). Consequently the molecular function is also highly
50 conserved in vertebrates, including fish (Ishibashi and Imai, 2002). In addition, mammalian
51
52
53
54
55
56
57
58
59
60

1
2
3 *STCI* is widely expressed in various tissues including the heart (Guo *et al.*, 2013; Yeung *et al.*,
4 2012), similar to zebrafish in the current study. Clinically, *STCI* is upregulated in the hearts of
5 patients with myocardial infarction and idiopathic dilated cardiomyopathy (Guo *et al.*, 2012).
6
7 However, it remains unclear whether downregulation of *STCI* by sorafenib treatment is
8 associated with ROS generation in cardiomyocytes as a mechanism of cardiotoxicity of
9 sorafenib.
10

11
12
13
14
15
16 Liu *et al.* have reported that human *STCI* activates a novel antioxidant pathway in
17 cardiomyocytes through induction of uncoupling protein 3 (UCP3), suggesting that *STCI*
18 plays an important role in suppressing ROS in the heart (Liu *et al.*, 2012). In our study,
19 reduction of *STCI* activated ROS production in human cardiomyocytes. Nguyen *et al.* also
20 have reported that the expression of *stc1* is positively regulated by ERK signaling (Nguyen *et*
21 *al.*, 2009). Therefore, sorafenib might induce overproduction of ROS caused by *STCI*
22 downregulation, through inhibition of ERK signaling, resulting in cytotoxic effects in both
23 zebrafish heart and human cardiomyocytes.
24
25
26
27
28
29
30
31
32

33
34 Finally, we performed forced expression of *stc1* to rescue the ventricular dysfunction
35 in zebrafish treated with sorafenib. To normalize expression level of *stc1* in zebrafish treated
36 with sorafenib, we injected *stc1* mRNA into zebrafish eggs and then treated them with 1 μ M
37 sorafenib from 72 to 96 hpf. We found that the forced expression of *stc1* in zebrafish with
38 sorafenib treatment normalized the decreasing longitudinal ventricular dimensions caused by
39 sorafenib treatment. Consequently, these studies suggest that *STCI* plays a role in protection
40 against oxidative stress by ROS overproduction in cardiomyocytes following sorafenib
41 treatment.
42
43
44
45
46
47
48
49
50

51
52 In conclusion, we established that *STCI* downregulation is responsible for
53 sorafenib-induced cardiotoxicity through activated ROS generation.
54
55
56
57
58
59
60

SUPPLEMENTARY DATA

Supplementary data are available online at <http://toxsci.oxfordjournals.org/>.

FUNDING

This work was supported in part by grants from Mie University Graduate School of Medicine; the Ministry of Education, Culture, Sports, Science and Technology (MEXT) of Japan; the Japan Science and Technology Agency; the Long-range Research Initiative of the Japan Chemical Industrial Association; the Johns Hopkins Center for Alternatives to Animal Testing; and the Sumitomo Foundation.

ACKNOWLEDGMENTS

We express our gratitude to Dr. K. Dohi and Dr. K. Miyashita for helpful discussions, and T. Oka for teaching us bioinformatics analysis. We are grateful to Dr. K. Kawakami (National Institute of Genetics, Japan) for providing the SAG4A line. We thank R. Kawase, S. Ichikawa, M. Ariyoshi, H. Nakayama and J. Koiwa for zebrafish breeding, and R. Ikeyama and Y. Tamura for secretarial assistance.

Conflict of Interest: none declared.

Figure legends

Figure 1. Assessment of general toxicity of sorafenib in MK009 zebrafish. (A). Survival rate of MK009 treated with or without sorafenib (1 or 3 μ M) from 3 to 10 dpf. Viable MK009 were counted daily from 3 dpf. Fifty zebrafish per group were analyzed.

(B). Treatment with 3 μ M sorafenib from 72 to 96 hpf caused pericardial edema in MK009. MK009 treated with or without 1 μ M sorafenib did not show pericardial edema or any external malformation. Scale bar: 200 μ m.

Figure 2. Sorafenib cardiotoxicity in MK009 zebrafish. MK009 were treated with or without 1 μ M sorafenib from 72 to 96 or 120 hpf. Functional cardiac imaging was performed at 96 or 120 hpf. (A) Assessment of VDs or VDd of both short and long axes at 96 hpf. (B) Calculated EF and FS based on VDd and VDs at 96 hpf. (A and B) (control, $n = 9$; sorafenib, $n = 13$). $**P < 0.01$. (C) Assessment of VDs or VDd of both short and long axes at 120 hpf. (D) Calculated EF and FS based on VDd and VDs at 120 hpf. (C and D) (control, $n = 10$; sorafenib, $n = 12$). $**P < 0.01$.

Figure 3. Reduction of *stc1* expression caused a significant decrease in ventricular dimension. (A and B) qPCR to assess *stc1* (*STC1*) expression. (A) MK009 were treated with or without 1 μ M sorafenib from 72 to 96 hpf. The hearts were isolated from these zebrafish and qPCR was performed to assess the expression of *stc1*. $*P < 0.05$, zebrafish treated with sorafenib versus zebrafish without sorafenib treatment. Four samples per group were analyzed. One sample contained 20 hearts of zebrafish. (B) Human cardiomyocytes were treated with or without 0.3 μ M sorafenib for 24 hours. qPCR was performed to assess the expression of *STC1*. $*P < 0.05$. Four samples per group were analyzed. (C) MK009 at 1–4-cell stages were injected with 0.3

1
2
3 mM *stc1* MO and raised to 96 hpf. Total RNA was extracted from the whole body and qPCR
4
5 was performed to assess expression of *stc1*. ** $P < 0.01$, zebrafish injected with *stc1* MO
6
7 versus zebrafish injected with control MO. Eight zebrafish per group were analyzed. (D and
8
9 *E*): Assessment of cardiac function in zebrafish injected with control MO, *stc1* MO or *stc1*
10
11 MO and *stc1* mRNA. Twenty zebrafish per group were analyzed. For multiple comparisons,
12
13 one-way analysis of variance followed by the Tukey–Kramer procedure was used. (*D*)
14
15 Assessment of VDs or VDd of both short and long axes. (*E*) Calculated EF and FS based on
16
17 VDd and VDs. * $P < 0.05$
18
19
20
21
22

Figure 4. ROS overproduction in zebrafish treated with sorafenib, or injected with *stc1* MO.
23
24 ROS was detected using DHE. Images were performed at 74 hpf. (*A*) Typical images of
25
26 zebrafish treated with vehicle, 1 μ M sorafenib, 1 μ M sorafenib + 5 mM NAC for 2 hours.
27
28 Scale bar: 500 μ m. (*B*) Quantitative analysis of ROS in the zebrafish. (n=15), * $P < 0.05$, ** P
29
30 < 0.01 . (*C*) Typical images of zebrafish injected with 0.3 mM control MO, 0.3 mM *stc1* MO,
31
32 0.3 mM *stc1* MO + 5 mM NAC. Scale bar: 500 μ m. (*D*) Quantitative analysis of ROS in the
33
34 zebrafish. (Control MO, $n = 8$; *stc1* MO, $n = 10$; *stc1* MO+NAC, $n=6$), * $P < 0.05$. (*E*)
35
36 Quantitative analysis of ROS in the zebrafish injected with 0.3 mM control MO, 0.3 mM *stc1*
37
38 MO, 0.3 mM *stc1* MO + *stc1* mRNA.. (n=10), ** $P < 0.01$.
39
40
41
42
43
44

Figure 5. ROS overproduction in human cardiomyocytes treated with sorafenib, or
45
46 transfected with STC1siRNA. ROS and nuclei were detected using CellRox dyes (red) and
47
48 Hoechst 33342 (blue), respectively. (*A*) Typical images of cardiomyocytes treated with
49
50 vehicle, 0.3 μ M sorafenib, 0.3 μ M sorafenib + 5 mM NAC for 1 hour. Scale bar: 100 μ m. (*B*)
51
52 Quantitative analysis of ROS in the cells. (control, $n =8$; sorafenib, $n =8$; sorafenib+NAC, n
53
54 $=5$), * $P < 0.05$, ** $P < 0.01$. (*C*) Typical images of cardiomyocytes transfected with NC
55
56
57
58
59
60

1
2
3 siRNA and STC1siRNAs. Cultured cells were transfected with siRNAs. Scale bar: 100 μ m.
4
5 (D) Quantitative analysis of ROS in the cells. (n=4), $**P < 0.01$. (E) Human cardiomyocytes
6
7 were transfected with NCsiRNA and STC1siRNAs. qPCR was performed to assess expression
8
9 of *STC1*. $*P < 0.05$, cardiomyocytes with STC1siRNA versus cardiomyocytes with negative
10
11 control. Three samples per group were analyzed.
12
13

14
15
16
17
18 **Figure 6.** Forced expression of *stc1* mRNA reversed sorafenib-induced cardiotoxicity. (A and
19
20 B) MK009 zebrafish at 1–4-cell stages were injected with or without *stc1* mRNA and treated
21
22 with or without 1 μ M sorafenib from 72 to 96 hpf. Functional cardiac imaging was performed
23
24 at 96 hpf. (A) Assessment of VDs or VDd of both short and long axes. (B) Calculated EF and
25
26 FS based on VDd and VDs. Seventeen zebrafish per group were analyzed. $*P < 0.05$, $**P <$
27
28 0.01. (C) Quantitative analysis of ROS in the zebrafish. MK009 zebrafish at 1–4-cell stages
29
30 were injected with or without *stc1* mRNA and treated with or without 1 μ M sorafenib from 72
31
32 to 74 hpf. Thirteen zebrafish per group were analyzed. $*P < 0.05$, $**P < 0.01$. (A, B and C)
33
34 For multiple comparisons, one-way analysis of variance followed by the Tukey–Kramer
35
36 procedure was used.
37
38
39
40
41
42

43 **Supplemental figure legends**

44
45 **Table S1.** Sequences of primers, MOs and siRNAs.
46
47

48
49
50 **Table S2.** Genes dysregulated in the heart of zebrafish treated with sorafenib from 72 to 96
51
52 hpf.
53
54
55
56
57
58
59
60

1
2
3 **Table S3.** Genes ontology list of dysregulated in the hearts by sorafenib treatment in Pathway
4
5 Studio.

6
7
8
9 **Figure S1.** Zebrafish imaging

10
11 (A) Bright field and fluorescence image of SAG4A and MK009.

12
13 (B) Functional cardiac imaging used in this study. (A) Fluorescent imaging of MK009 at 96
14 hpf. The heart expressing GFP is shown in the rectangle. (B) VD_s and VD_d were measured
15
16 from the M-mode images at both long and short axes.
17
18
19

20
21
22 **Figure S2.** (A and B) Genes dysregulated in the hearts by sorafenib treatment and linked to
23 heart failure in Pathway Studio. (C) There was no significant difference in the ROS
24 generation after 48 h exposure (1 uM sorafenib). Ten zebrafish per group were analyzed. (D)
25
26 The *stc I* gene expression was significantly increased after 48 h exposure (1 uM sorafenib).
27
28 Seven zebrafish per group were analyzed.
29
30
31
32
33
34
35
36
37
38
39
40
41
42
43
44
45
46
47
48
49
50
51
52
53
54
55
56
57
58
59
60

References

Adão, R., de Keulenaer, G., Leite-Moreira, A., and Brás-Silva, C. (2013). Cardiotoxicity associated with cancer therapy: pathophysiology and prevention strategies. *Rev. Port. Cardiol.* **32**, 395-409.

Berthiaume, J. M., and Wallace, K. B. (2007). Adriamycin-induced oxidative mitochondrial cardiotoxicity. *Cell Biol. Toxicol.* **23**, 15-25.

Bruix, J., Sherman, American Association for the Study of Liver Diseases. (2011). Management of hepatocellular carcinoma: an update. *Hepatology* **53**, 1020-1022.

Burns, C. G., and MacRae, C. A. (2006). Purification of hearts from zebrafish embryos. *Biotechniques* **40**, 274-278.

Cheng, A. L., Kang, Y. K., Chen, Z., Tsao, C. J., Qin, S., Kim, J. S., Luo, R., Feng, J., Ye, S., Yang, T. S., Xu, J., Sun, Y., Liang, H., Liu, J., Wang, J., Tak, W. Y., Pan, H., Burock, K., Zou, J., Voliotis, D., and Guan, Z. (2009). Efficacy and safety of sorafenib in patients in the Asia-Pacific region with advanced hepatocellular carcinoma: a phase III randomised, double-blind, placebo-controlled trial. *Lancet Oncol.* **10**, 25-34.

Cheng, H., Kari, G., Dicker, A. P., Rodeck, U., Koch, W. J., and Force, T. (2011). A novel preclinical strategy for identifying cardiotoxic kinase inhibitors and mechanisms of cardiotoxicity. *Circ. Res.* **109**, 1401-1409.

Chiou, J. F., Tai, C. J., Wang, Y. H., Liu, T. Z., Jen, Y. M., and Shiau, C. Y. (2009). Sorafenib induces preferential apoptotic killing of a drug- and radio-resistant Hep G2 cells through a mitochondria-dependent oxidative stress mechanism. *Cancer Biol. Ther.* **8**, 1904-13.

Collins, T. J. (2007). ImageJ for microscopy. *Biotechniques* **43**, 25-30.

Coriat, R., Nicco, C., Chéreau, C., Mir, O., Alexandre, J., Ropert, S., Weill, B., Chaussade, S., Goldwasser, F., and Batteux, F. (2012). Sorafenib-induced hepatocellular carcinoma cell death

1
2
3 depends on reactive oxygen species production in vitro and in vivo. *Mol. Cancer Ther.* **11**,
4
5 2284-2293.

6
7 Di Salvo, G., Di Bello, V., Salustri, A., Antonini-Canterin, F., La Carrubba, S., Materazzo, C.,
8
9 Badano, L., Caso, P., Pezzano, A., Calabrò, R., Carerj, S., and Research Group of the Italian
10
11 Society of Cardiovascular Echography. (2011). The prognostic value of early left ventricular
12
13 longitudinal systolic dysfunction in asymptomatic subjects with cardiovascular risk factors.
14
15 *Clin Cardiol* **34**, 500-506.

16
17
18 Feng, X., Sun, T., Bei, Y., Ding, S., Zheng, W., Lu, Y., and Shen, P. (2013). S-nitrosylation of
19
20 ERK inhibits ERK phosphorylation and induces apoptosis. *Sci. Rep.* **3**, 1814.

21
22
23 Force, T., and Kolaja, K. L. (2011). Cardiotoxicity of kinase inhibitors: the prediction and
24
25 translation of preclinical models to clinical outcomes. *Nat. Rev. Drug Discov.* **10**, 111-126.

26
27 Force, T., Krause, D. S., and Van Etten, R. A. (2007). Molecular mechanisms of cardiotoxicity
28
29 of tyrosine kinase inhibition. *Nat. Rev. Cancer* **7**, 332-344.

30
31
32 Fumarola, C., Caffarra, C., La Monica, S., Galetti, M., Alfieri, R. R., Cavazzoni, A., Galvani,
33
34 E., Generali, D., Petronini, P. G., and Bonelli, M. A. (2013). Effects of sorafenib on energy
35
36 metabolism in breast cancer cells: role of AMPK-mTORC1 signaling. *Breast Cancer Res.*
37
38 *Treat.* **141**, 67-78.

39
40
41 Guo, F., Li, Y., Wang, J., and Li, G. (2013). Stanniocalcin1 (STC1) inhibits cell proliferation
42
43 and invasion of cervical cancer cells. *PLoS One* **8**, e53989.

44
45 Hasinoff, B. B., and Patel, D. (2010). Mechanisms of myocyte cytotoxicity induced by the
46
47 multikinase inhibitor sorafenib. *Cardiovasc. Toxicol.* **10**, 1-8.

48
49 Holmes, D. I., and Zachary, I. C. (2008). Vascular endothelial growth factor regulates
50
51 stanniocalcin-1 expression via neuropilin-1-dependent regulation of KDR and synergism with
52
53 fibroblast growth factor-2. *Cell Signal.* **20**, 569-579.

54
55
56 Ishibashi, K., and Imai, M. (2002). Prospect of a stanniocalcin endocrine/paracrine system in
57
58

1
2
3 mammals. *Am. J. Physiol. Renal Physiol.* **282**, F367-F375.

4
5 Jacob, E., Drexel, M., Schwerte, T., and Pelster, B. (2002). Influence of hypoxia and of
6
7 hypoxemia on the development of cardiac activity in zebrafish larvae. *Am. J. Physiol. Regul.*
8
9 *Integr. Comp. Physiol.* **283**, R911-R917.

10
11 Jiang, W. Q., Chang, A. C., Satoh, M., Furuichi, Y., Tam, P. P., and Reddel, R. R. (2000). The
12
13 distribution of stanniocalcin 1 protein in fetal mouse tissues suggests a role in bone and
14
15 muscle development. *J. Endocrinol.* **165**, 457-466.

16
17 Kawakami, K., Takeda, H., Kawakami, N., Kobayashi, M., Matsuda, N., and Mishina, M.
18
19 (2004). A transposon-mediated gene trap approach identifies developmentally regulated genes
20
21 in zebrafish. *Dev. Cell* **7**, 133-144.

22
23 Koizumi, K., Hoshiai, M., Ishida, H., Ohyama, K., Sugiyama, H., Naito, A., Toda, T.,
24
25 Nakazawa, H., and Nakazawa, S. (2007). Stanniocalcin 1 prevents cytosolic Ca²⁺ overload
26
27 and cell hypercontracture in cardiomyocytes. *Circ. J.* **71**, 796-801.

28
29 Lal, H., Kolaja, K. L., and Force, T. (2013). Cancer genetics and the cardiotoxicity of the
30
31 therapeutics. *J. Am. Coll. Cardiol.* **61**, 267-274.

32
33 Lister, J. A., Robertson, C. P., Lepage, T., Johnson, S. L., and Raible, D. W. (1999). nacre
34
35 encodes a zebrafish microphthalmia-related protein that regulates neural-crest-derived
36
37 pigment cell fate. *Development* **126**, 3757-3767.

38
39 Liu, D., Huang, L., Wang, Y., Wang, W., Wehrens, X. H., Belousova, T., Abdelrahim, M.,
40
41 DiMattia, G., and Sheikh-Hamad, D. (2012). Human stanniocalcin-1 suppresses angiotensin
42
43 II-induced superoxide generation in cardiomyocytes through UCP3-mediated anti-oxidant
44
45 pathway. *PLoS One* **7**, e36994.

46
47 Llovet, J. M., Di Bisceglie, A. M., Bruix, J., Kramer, B. S., Lencioni, R., Zhu, A. X.,
48
49 Sherman, M., Schwartz, M., Lotze, M., Talwalkar, J., Gores, G. J., and Panel of Experts in
50
51 HCC-Design Clinical Trials. (2008b). Design and endpoints of clinical trials in hepatocellular
52
53
54
55
56
57
58
59
60

1
2
3 carcinoma. *J Natl Cancer Inst* **100**, 698-711.

4
5 Llovet, J. M., Ricci, S., Mazzaferro, V., Hilgard, P., Gane, E., Blanc, J. F., de Oliveira, A. C.,
6
7 Santoro, A., Raoul, J. L., Forner, A., Schwartz, M., Porta, C., Zeuzem, S., Bolondi, L., Greten,
8
9 T. F., Galle, P. R., Seitz, J. F., Borbath, I., Häussinger, D., Giannaris, T., Shan, M., Moscovici,
10
11 M., Voliotis, D., Bruix, J., and Group, S. I. S. (2008a). Sorafenib in advanced hepatocellular
12
13 carcinoma. *N. Engl. J. Med.* **359**, 378-390.

14
15
16 Mellor, H. R., Bell, A. R., Valentin, J. P., and Roberts, R. R. (2011). Cardiotoxicity associated
17
18 with targeting kinase pathways in cancer. *Toxicol. Sci.* **120**, 14-32.

19
20
21 Miyahara, K., Nouse, K., and Yamamoto, K. (2014). Chemotherapy for advanced
22
23 hepatocellular carcinoma in the sorafenib age. *World J. Gastroenterol.* **20**, 4151-4159.

24
25 Nguyen, A., Chang, A. C., and Reddel, R. R. (2009). Stanniocalcin-1 acts in a negative
26
27 feedback loop in the prosurvival ERK1/2 signaling pathway during oxidative stress.
28
29 *Oncogene* **28**, 1982-1992.

30
31 Ogrunc, M., Di Micco, R., Liontos, M., Bombardelli, L., Mione, M., Fumagalli, M.,
32
33 Gorgoulis, V. G., and d'Adda di Fagagna, F. (2014). Oncogene-induced reactive oxygen
34
35 species fuel hyperproliferation and DNA damage response activation. *Cell Death Differ.* **21**,
36
37 998-1012.

38
39
40 Orphanos, G. S., Ioannidis, G. N., and Ardavanis, A. G. (2009). Cardiotoxicity induced by
41
42 tyrosine kinase inhibitors. *Acta Oncol.* **48**, 964-970.

43
44
45 Roux, P. P., and Blenis, J. (2004). ERK and p38 MAPK-activated protein kinases: a family of
46
47 protein kinases with diverse biological functions. *Microbiol. Mol. Biol. Rev.* **68**, 320-344.

48
49 Schmidinger, M., Zielinski, C. C., Vogl, U. M., Bojic, A., Bojic, M., Schukro, C., Ruhsam,
50
51 M., Hejna, M., and Schmidinger, H. (2008). Cardiac toxicity of sunitinib and sorafenib in
52
53 patients with metastatic renal cell carcinoma. *J. Clin. Oncol.* **26**, 5204-5212.

54
55
56 Seguchi, O., Takashima, S., Yamazaki, S., Asakura, M., Asano, Y., Shintani, Y., Wakeno, M.,
57
58
59
60

1
2
3 Minamino, T., Kondo, H., Furukawa, H., Nakamaru, K., Naito, A., Takahashi, T., Ohtsuka, T.,
4 Kawakami, K., Isomura, T., Kitamura, S., Tomoike, H., Mochizuki, N., and Kitakaze, M.
5 (2007). A cardiac myosin light chain kinase regulates sarcomere assembly in the vertebrate
6 heart. *The Journal of Clinical Investigation*. **117**, 2812-2824.
7

8
9
10
11 Strumberg, D., Clark, J. W., Awada, A., Moore, M. J., Richly, H., Hendlisch, A., Hirte, H. W.,
12 Eder, J. P., Lenz, H., and Schwartz, B. (2007). Safety, pharmacokinetics, and preliminary
13 antitumor activity of sorafenib: A review of four phase 1 trials in patients with advanced
14 refractory solid tumors. *The Oncologist*, **12**, 426-437.
15

16
17
18
19
20 Tolcher, A. W., Appleman, L. J., Shapiro, G. I., Mita, A. C., Cihon, F., Mazzu, A., and
21 Sundaresan, P. R. (2011). A phase I open-label study evaluating the cardiovascular safety of
22 sorafenib in patients with advanced cancer. *Cancer Chemother. Pharmacol.* **67**, 751-764.
23

24
25
26
27 Umemoto, N., Nishimura, Y., Shimada, Y., Yamanaka, Y., Kishi, S., Ito, S., Okamori, K.,
28 Nakamura, Y., Kuroyanagi, J., Zhang, Z., Zang, L., Wang, Z., Nishimura, N., and Tanaka, T.
29 (2013). Fluorescent-based methods for gene knockdown and functional cardiac imaging in
30 zebrafish. *Mol. Biotechnol.* **55**, 131-142.
31

32
33
34
35
36 Westerfield, M. (2007). *The Zebrafish Book, a Guide for the Laboratory Use of Zebrafish*
37
38 (*Danio rerio*), 4th ed. University of Oregon Press, Eugene, OR.
39

40
41
42
43
44
45
46
47
48
49
50
51
52
53
54
55
56
57
58
59
60
Yeung, B. H., Law, A. Y., and Wong, C. K. (2012). Evolution and roles of stanniocalcin. *Mol. Cell Endocrinol.* **349**, 272-280.

1
2
3
4
5
6
7
8
9
10
11
12
13
14
15
16
17
18
19
20
21
22
23
24
25
26
27
28
29
30
31
32
33
34
35
36
37
38
39
40
41
42
43
44
45
46
47
48
49
50
51
52
53
54
55
56
57
58
59
60

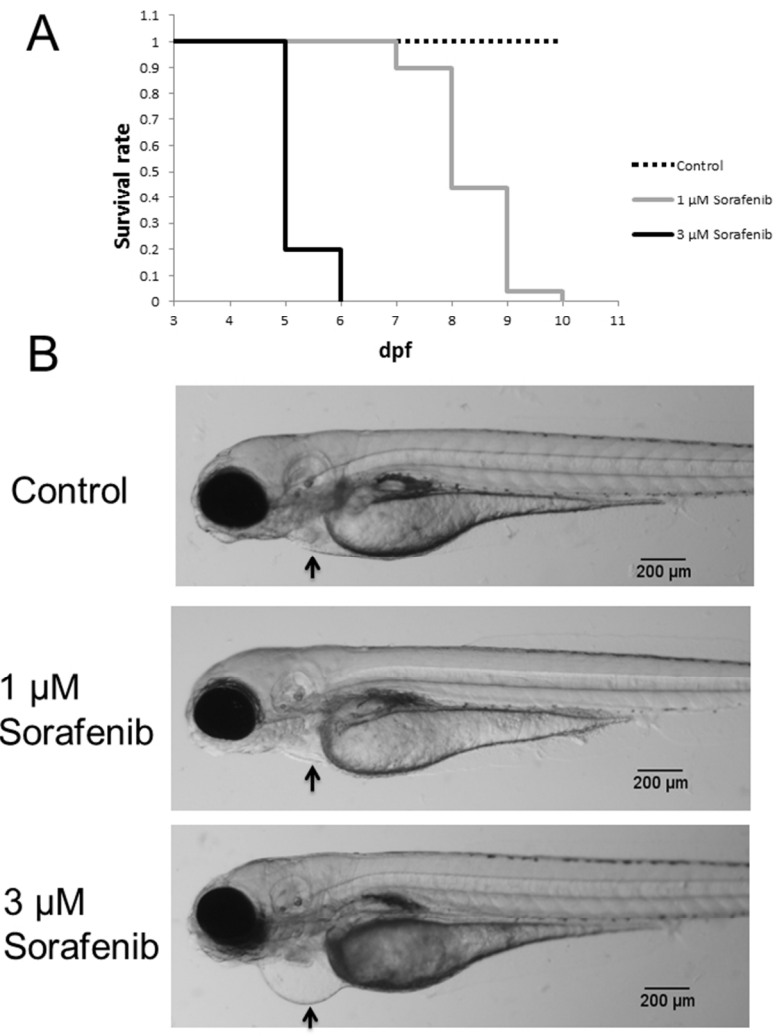


Figure 1

190x275mm (96 x 96 DPI)

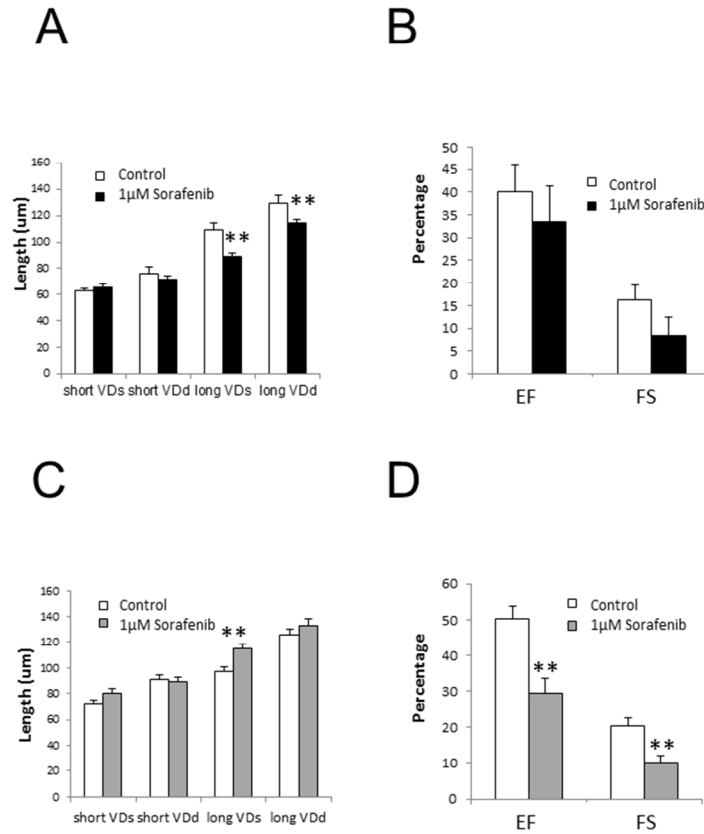


Figure 2

190x275mm (96 x 96 DPI)

1
2
3
4
5
6
7
8
9
10
11
12
13
14
15
16
17
18
19
20
21
22
23
24
25
26
27
28
29
30
31
32
33
34
35
36
37
38
39
40
41
42
43
44
45
46
47
48
49
50
51
52
53
54
55
56
57
58
59
60

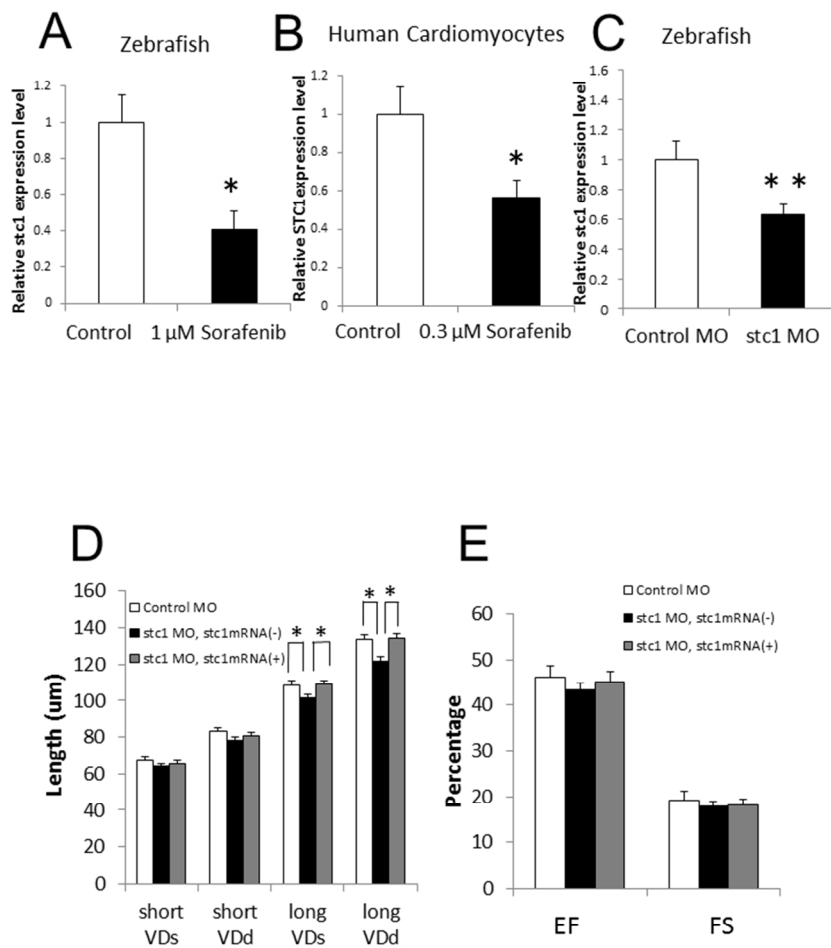


Figure 3

190x275mm (96 x 96 DPI)

1
2
3
4
5
6
7
8
9
10
11
12
13
14
15
16
17
18
19
20
21
22
23
24
25
26
27
28
29
30
31
32
33
34
35
36
37
38
39
40
41
42
43
44
45
46
47
48
49
50
51
52
53
54
55
56
57
58
59
60

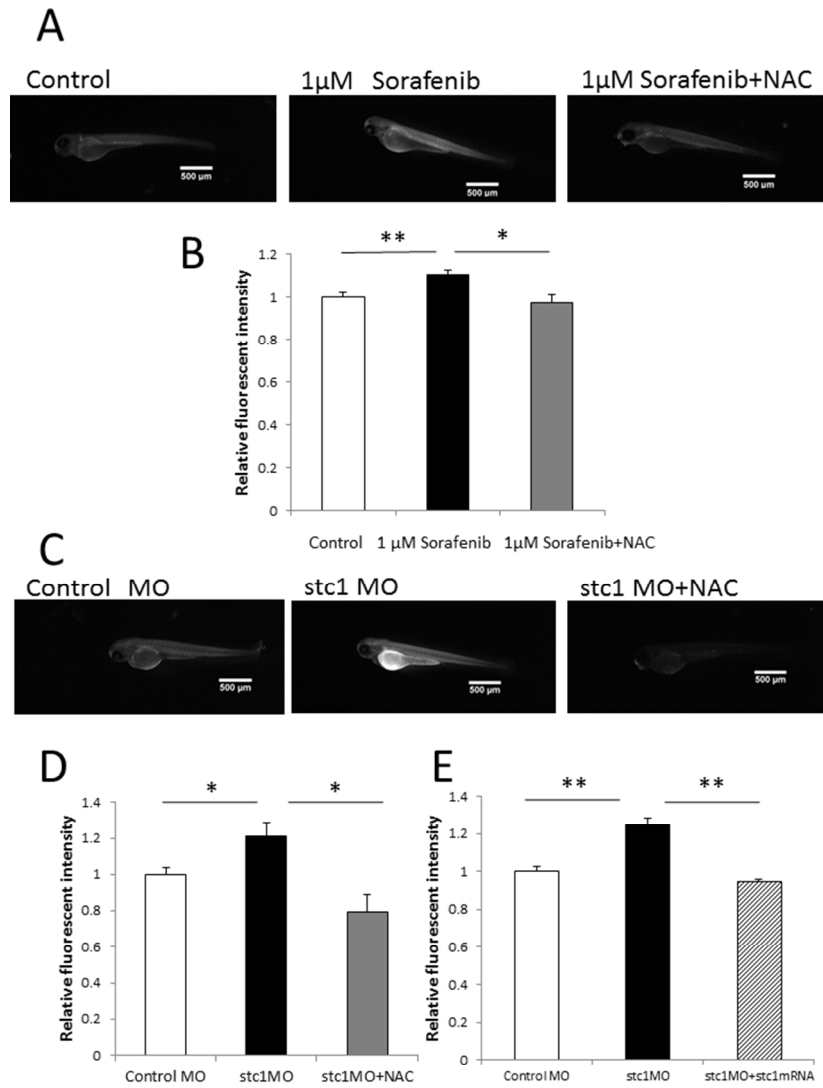


Figure 4

190x275mm (96 x 96 DPI)

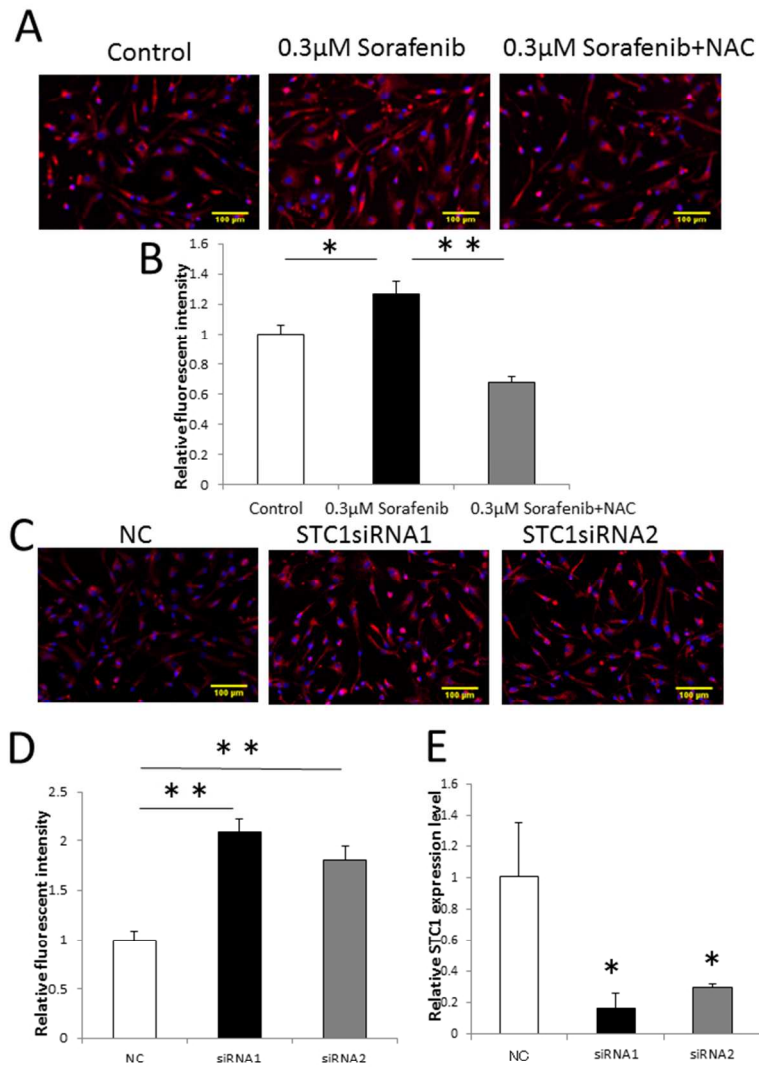


Figure 5

190x275mm (96 x 96 DPI)

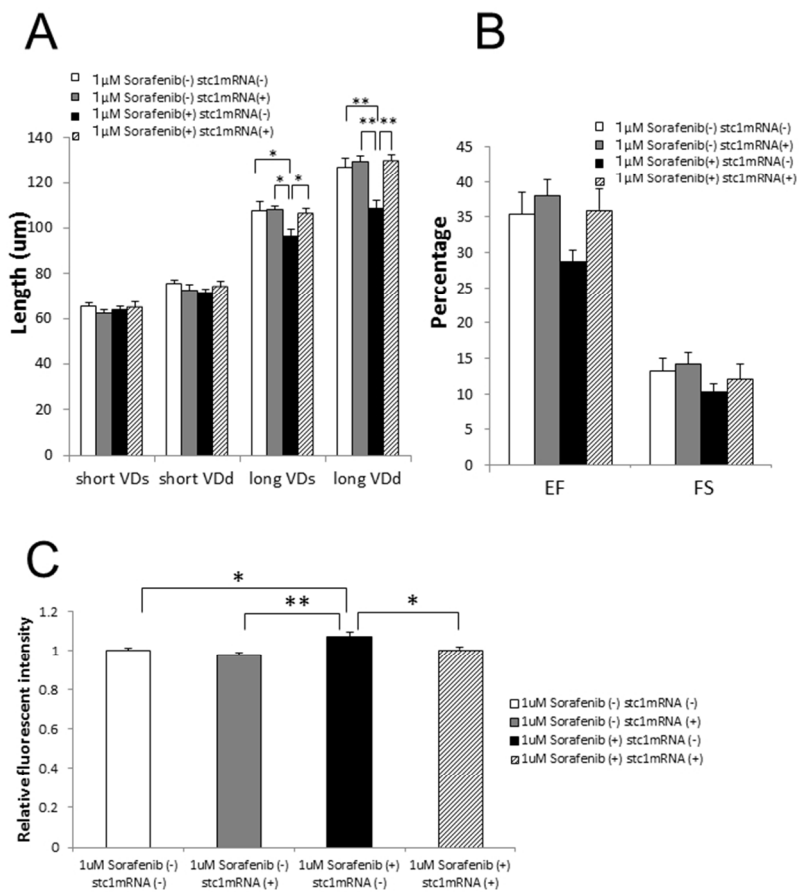


Figure 6

190x275mm (96 x 96 DPI)

1
2
3
4
5
6
7
8
9
10
11
12
13
14
15
16
17
18
19
20
21
22
23
24
25
26
27
28
29
30
31
32
33
34
35
36
37
38
39
40
41
42
43
44
45
46
47
48
49
50
51
52
53
54
55
56
57
58
59
60